JOURNAL OF CATALYSIS 14, 93–103 (1969)

Structure–Catalytic Efficiency Relationships in U–Sb Oxide Acrylonitrile Synthesis Catalysts*

R. K. GRASSELLI AND J. L. CALLAHAN

From the Research and Development Department, The Standard Oil Company (Ohio), Cleveland, Ohio 44128

Received June 24, 1968; revised January 14, 1969

A novel uranium–antimony oxide catalyst which has recently entered full-scale commercial production and use is shown to be highly effective for the direct oxidation of propylene-ammonia to acrylonitrile. Direct single-step conversion of propylene feed to acrylonitrile in excess of 80% was achieved in a laboratory-scale fluidized-bed reactor. Approximately 6% of the propylene is converted to HCN, less than 1% to acetonitrile, and only traces to condensable oxygenated organics.

The interdependence of catalytic efficiency, catalyst crystalline structure, low-frequency infrared spectral characteristics, electron spin resonance behavior, and catalyst composition is discussed. Antimony-uranium containing crystalline phases were identified and correlated to effectiveness in acrylonitrile synthesis.

INTRODUCTION

The discovery of means for the direct catalytic oxidation of propylene and ammonia to acrylonitrile (*1*, *2*) has had a far reaching impact on the production of this monomer. Since 1960, when the first commercial plant of this type went on stream, the world acrylonitrile capacity has grown from 400 million pounds/year to a current estimated 1800 million pounds/year. More significantly, almost all of this new capacity is based on propylene ammoxidation technology.

The most widely used catalyst for acrylonitrile synthesis has been bismuth phosphomolybdate (*3*). Because of the technical importance of this catalyst in oxidative synthesis, it has been the subject of a growing number of important investigations (*4–14*).

The purpose of this paper is to report the properties and catalytic behavior of a new, more efficient, oxidative acrylonitrile synthesis catalyst which has just recently been brought into full commercial use. The commercial catalyst is comprised of silica-supported complex antimony–uranium oxides (*15*, *16*). However, in the work to be reported, much of the experimentation was performed upon unsupported antimony–uranium oxides. The catalyst possesses high activity and selectivity in both the supported and unsupported form, although the highly attrition resistant supported form (*17*) is much preferred for commercial operation in fluidized-bed reactors.

EXPERIMENTAL

The silica-supported catalyst was prepared by combining 484.5 g Sb_2O_3, 365 g $UO_2(NO_3)_2 \cdot 6H_2O$, 1490 g 70% HNO_3, and 146 ml distilled water under reflux (110°C) for 3 hr. After cooling, 427 g of duPont Ludox AS (30 wt % SiO_2 sol) was added to the slurry followed by adjustment of the pH to 8.0 with 28% NH_4OH. The resulting slurry was filtered, dried at 130°C for 8 hr, heated at 430°C for 3 hr to decompose nitrates, and finally heated at 940°C for 2 hr. The solid product (847.2 g) was ball-milled with 1170 g duPont Ludox AS to yield a smooth suspension which was dried at 110°C, heated for 2 hr at 940°C, and ground and screened to yield a 20 to 100 μ size fraction. The final composition of this catalyst was 60 wt % $USb_{4.6}O_{12.2}$–40 wt % SiO_2.

A typical unsupported catalyst was prepared by combining 80.3 g Sb_2O_3, 60.2 g

---

* Presented at the Symposium on "New Reactions in Chemical Processes," 155th National ACS Meeting, San Francisco, California, April 3, 1968.

$UO_2(NO_3)_2 \cdot 6H_2O$, 321.0 ml 70% HNO_3, and 100 ml H_2O at reflux for 3 hr. The product was cooled, brought to a pH of 8 by addition of 28% NH_4OH, filtered, dried at 120°C for 24 hr, heated at 427°C for 16 hr and finally brought to 927°C for 16 hr. The final composition of this catalyst was $USb_{4.6}O_{12.2}$ (elemental analysis gave a U/Sb atom ratio of 1/4.54).

Preparations of other unsupported catalysts of varying U/Sb ratio were identical to the method outlined above, except for the weight of uranyl nitrate.

Catalytic activity tests were conducted in both fixed-bed and fluidized-bed reactors.

The unsupported catalysts were tested in an upflow fixed-bed microreactor. The reactor consisted of a 15 cm length of 0.78-cm id stainless steel tube, with an inlet port of 0.30-cm id at the bottom, a porous stainless steel catalyst support plate 1.1 cm from the bottom, and a removable top, telescoped down to a 0.11-cm id tube which served as the outlet port.

The reactor contained 4 cm^3 of 500 to 840 μ size catalyst particles and was submerged in a molten salt bath whose temperature was controlled to within ±1°C.

The premixed feed gases were metered to the reactor by means of flow control devices. The effluent gases were scrubbed in a microscrubber containing 5 cm^3 of 0.5 N HCl solution. The condensable as well as noncondensable gases were analyzed by standard gas chromatographic techniques.

Throughout this study the following notations are used:

$$\text{Percent conversion} = \frac{\text{G atoms of carbon in product}}{\text{G atoms of carbon in propylene feed}} \times 100$$

Percent selectivity (Acrylonitrile)

$$= \frac{\text{Mole acrylonitrile produced}}{\text{Mole propylene converted}} \times 100$$

Superficial contact time (sec)

$$= \frac{\text{Catalyst bulk volume (cm}^3)}{\text{Flow rate of feed gas at reaction temperature (cm}^3\text{/sec)}} \times 100$$

Fluidized-bed tests on supported catalysts were performed in a reactor fabricated from $1\frac{1}{2}$-inch schedule 40 carbon steel pipe, 24 inches in length. Air feed entered the reactor at the bottom through a sintered stainless steel sparger plate. Propylene and ammonia feed were mixed external to the reactor and were sparged into the fluidized catalyst bed at a point $4\frac{1}{2}$ inches above the air sparger. Effluent passed from the reactor through a stainless steel bayonet filter to prevent loss of entrained catalyst. Temperature control was accomplished by immersion of the entire reactor in a molten salt bath. Condensible products were absorbed in dilute HCl, which neutralized unreacted ammonia. Fixed gases were metered and sampled for analysis.

The absorber solution was analyzed on a 6 ft × $\frac{1}{8}$ inch Porapak Q column programmed between 130° and 220°C using a flame-ionization detector (F & M Vapor Fractometer 5754-A). This system quantitatively detected acrylonitrile, acetonitrile, acrolein, acetone, and acetaldehyde. HCN and ammonia in the absorber solution were determined by standard titration methods.

Fixed gases (CO, CO_2, propylene, O_2, and N_2) were analyzed by a Fisher Gas Partitioner at 30°C using two columns in series. The first column was 6 ft × $\frac{1}{4}$ inch 30% hexamethyl phosphoramide on 60–80 mesh Chromosorb P; the second column was a 12 ft × $\frac{1}{4}$ inch combination of 5 ft of uncoated Columnpak followed by 7 ft of molecular sieves 13X.

X-Ray diffraction patterns were obtained on catalyst samples, ground to $<44\text{-}\mu$ particle size, using Cu $K\alpha$ radiation (λ = 1.5418 Å) and a Ni filter. Each sample was scanned from $2\theta = 7°$ to 70° at a rate of 1°/min.

Low-frequency infrared absorption spectra of catalyst samples were obtained on a Perkin-Elmer 521 grating spectrophotom-

TABLE 1

ACTIVITY–SELECTIVITY OF UNSUPPORTED SB-U COMPOUNDS FOR PROPYLENE AMMOXIDATION

Temperature, 391°C
Superficial contact time, 3.0 sec
Feed ratios: Propylene/NH_3/Air = 1/1.2/12.0

Sb/U (atom ratio)	Propylene conversion (mole %) to—				Selectivity (Acrylonitrile)
	Acrylonitrile	CO_2 + CO	HCN	Total	
18.4/1	24.0	1.5	2.88	28.4	84.5
9.2/1	28.7	3.0	2.94	34.6	83.0
4.6/1	34.5	15.5	0.25	50.3	68.6
3.0/1	45.4	24.8	2.46	72.7	62.5
2.5/1	37.8	29.6	4.82	72.2	52.6
2.0/1	31.7	39.3	3.13	74.1	43.0
1.0/1.0	22.0	39.6	5.37	67.0	32.9

eter. Samples were ground <30-μ particle size and run as CsI pellets. The spectra were recorded from 1000 to 250 cm^{-1}.

ESR spectra of catalyst samples were recorded on a Varian E-2 instrument with scan range of $\pm 1 \times 10^4$ G, time constant of 0.1 sec, microwave power of 100 mW, field set 3400 G, scan time of 8 min, modulation frequency of 100 kc/sec ambient temperature, and microwave frequency of 9.535 Gc/sec.

RESULTS AND DISCUSSION

Tables 1 and 2 list catalytic activity test results on the conversion of propylene-ammonia to acrylonitrile secured for a series of varying Sb/U ratio unsupported catalysts at two reaction temperatures (391° and 460°C). While acrylonitrile is produced over a very wide range of compositions (Sb/U from 99/1 to 1/50), there is a marked optimum conversion efficiency in the Sb/U range of about 3/1. Figures 1 and 2 show these results graphically.

X-Ray diffraction data on these same catalyst samples are given in Table 3. In addition to Sb_2O_4 and U_3O_8, two crystalline phases not previously reported were identified. Phase I appears prominently at Sb/U of 2 and higher; Phase II reaches a maximum intensity at Sb/U of 1 but also is present at lower values of Sb/U. The intensity ratios (I/I_1) for the major unique lines of both Phase I and II remained substantially constant with variation of Sb/U composition, lending support to their assignment. The X-ray spectra of the catalyst samples before and after use were identical. X-Ray spectra of the catalyst compositions were also secured at reaction temperature (460°C) with no changes in the line positions or relative intensities observed.

The observed X-ray diffraction spectrum of essentially pure Phase I permitted assign-

TABLE 2

ACTIVITY–SELECTIVITY OF UNSUPPORTED SB-U COMPOUNDS FOR PROPYLENE AMMOXIDATION

Temperature, 460°C
Superficial contact time, 5.0 sec
Feed ratios: Propylene/NH_3/Air = 1/1.2/12

Sb/U (atom ratio)	Propylene conversion (mole %) to—				Selectivity (Acrylonitrile)
	Acrylonitrile	CO_2 + CO	HCN	Total	
18.4/1	67.8	19.6	3.39	90.8	74.6
9.2/1	65.0	19.8	4.53	89.3	72.8
4.6/1	74.3	20.8	0.2	95.3	78.0
3.5/1	61.3	26.3	4.57	92.2	66.5
3.0/1	62.0	30.8	2.41	95.2	65.2
2.5/1	47.4	37.4	2.53	87.3	54.3
2.0/1	47.8	33.6	4.5	85.9	55.6
1.0/1	33.0	42.8	3.93	79.7	41.4

TABLE 3

Summary of X-Ray Data of Unsupported Sb-U Catalysts

d(Å)	Mean relative intensity I/I_1	Sb/U (atom ratio)																							
		1/9.2		1/4.6		1/3		1/1.5		1/1		2/1		2.5/1		3/1		3.5/1		4.6/1		9.2/1		18.4/1	
		I	I/I_1	I	I/I_1	I	I/I_1	I	I/I_1	I	I/I_1	I	I/I_1	I	I/I_1	I	I/I_1	I	I/I_1	I	I/I_1	I	I/I_1	I	I/I_1
Phase I $(UO_2)Sb_3O_7$																									
5.89	7	—	—	—	—	—	—	—	—	—	—	16	5	37	8	28	6	28	7	19	6	16	6	16	8
3.85	66	—	—	—	—	—	—	—	—	—	—	262	77	296	68	330	68	271	67	214	67	164	63	103	54
3.18	100	—	—	—	—	—	—	—	—	—	—	342	100	437	100	488	100	406	100	325	100	261	100	192	100
2.45	59	—	—	—	—	—	—	—	—	—	—	205	60	243	56	288	59	236	58	201	62	161	62	106	55
1.920	12	—	—	—	—	—	—	—	—	—	—	42	12	45	15	54	11	49	12	40	12	33	13	23	12
1.834	25	—	—	—	—	—	—	—	—	—	—	86	25	88	20	125	25	106	26	90	28	70	27	49	25
1.657	29	—	—	—	—	—	—	—	—	—	—	105	31	115	26	138	28	113	28	96	30	94	36	46	24
1.645	31	—	—	—	—	—	—	—	—	—	—	107	31	133	30	155	32	131	32	109	33	87	33	51	26
1.589	15	—	—	—	—	—	—	—	—	—	—	43	13	54	12	67	14	58	14	54	17	45	17	35	18
1.468	19	—	—	—	—	—	—	—	—	—	—	64	19	71	16	87	18	74	18	71	22	61	23	64	33
Phase II $Sb_3U_3O_{14}$																									
5.04	12	10	10	19	14	29	12	60	13	19	14	10	9	9	13	—	—	—	—	—	—	—	—	—	—
3.95	61	49	50	90	66	144	61	284	64	360	64	64	59	44	61	—	—	—	—	—	—	—	—	—	—
3.41^a	4	4	4	6	4	10	4	17	4	22	4	4	4	3	4	—	—	—	—	—	—	—	—	—	—
3.26	100	97	100	136	100	236	100	443	100	577	100	104	100	72	100	—	—	—	—	—	—	—	—	—	—
2.51	63	52	54	92	68	156	66	291	66	388	69	63	61	43	60	—	—	—	—	—	—	—	—	—	—
1.975^a	21	14	15	39	29	59	25	85	19	94	16	20	21	18	25	—	—	—	—	—	—	—	—	—	—
1.886	12	9	9	17	13	28	12	53	12	59	11	—	—	—	—	—	—	—	—	—	—	—	—	—	—
1.875	14	10	10	20	15	34	14	65	15	81	15	16	15	10	14	—	—	—	—	—	—	—	—	—	—
1.691	58	57	59	87	65	144	61	248	56	317	57	60	58	37	52	—	—	—	—	—	—	—	—	—	—
1.630	9	7	7	15	11	22	10	41	9	50	9	—	—	—	—	—	—	—	—	—	—	—	—	—	—
1.507	17	23	24	25	18	41	17	66	15	78	14	14	13	—	—	—	—	—	—	—	—	—	—	—	—
1.360	16	—	—	25	18	37	16	67	15	88	16	16	15	—	—	—	—	—	—	—	—	—	—	—	—

												Sb_2O_4													
4.48	25	—	—	—	—	—	—	—	—	—	—	—	—	—	—	4	33	14	30	11	20	32	22	33	22
3.45	36	—	—	—	—	—	—	—	—	—	—	—	—	—	—	—	—	16	35	18	33	64	43	48	33
3.08	100	—	—	—	—	—	—	—	—	—	—	—	—	—	—	12	100	46	100	55	100	148	100	147	100
2.95	43	—	—	—	—	—	—	—	—	—	—	—	—	—	—	6	50	17	37	21	38	54	37	84	55
2.65	25	—	—	—	—	—	—	—	—	—	—	—	—	—	—	—	—	10	22	12	22	34	23	50	34
1.864	43	—	—	—	—	—	—	—	—	—	—	—	—	—	—	6	50	17	37	21	38	66	44	68	46
1.782	25	—	—	—	—	—	—	—	—	—	—	—	—	—	—	4	33	8	17	13	24	34	23	45	30
												U_3O_8													
4.18	100	328	100	228	100	150	100	73	100	10	100	—	—	—	—	—	—	—	—	—	—	—	—	—	—
3.41[a]	97	324	99	222	97	147	96	70	98	7	70	—	—	—	—	—	—	—	—	—	—	—	—	—	—
3.37	45	144	44	108	47	76	51	26	35	5	50	—	—	—	—	—	—	—	—	—	—	—	—	—	—
2.64	83	268	82	204	91	134	89	61	84	7	70	—	—	—	—	—	—	—	—	—	—	—	—	—	—
2.62	28	92	28	70	31	44	29	18	25	7	70	—	—	—	—	—	—	—	—	—	—	—	—	—	—
2.08	21	70	21	56	25	34	23	10	14	8	80	—	—	—	—	—	—	—	—	—	—	—	—	—	—
1.975[a]	20	66	20	46	20	34	23	10	14	2	20	—	—	—	—	—	—	—	—	—	—	—	—	—	—
1.956	19	54	16	40	18	27	18	17	23	13	—	—	—	—	—	—	—	—	—	—	—	—	—	—	—
1.793	29	84	25	80	35	42	28	21	29	—	—	—	—	—	—	—	—	—	—	—	—	—	—	—	—
1.77	74	208	63	165	72	104	69	59	81	—	—	—	—	—	—	—	—	—	—	—	—	—	—	—	—
1.583	20	46	14	40	18	30	20	22	30	14	—	—	—	—	—	—	—	—	—	—	—	—	—	—	—
1.422	11	32	10	28	12	17	11	—	—	—	—	—	—	—	—	—	—	—	—	—	—	—	—	—	—

[a] Lines common to Phase II and U_3O_8.

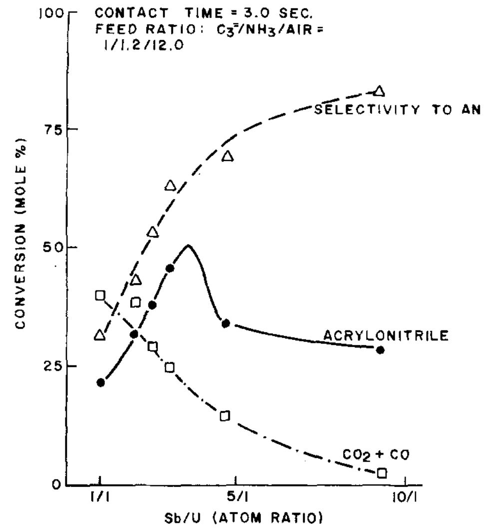

FIG. 1. Activity of unsupported Sb-U-catalysts at 391°C.

ment of 15 unique lines while that of essentially pure Phase II permitted an assignment of 44 unique lines. These data are given in Table 4. The major X-ray diffraction lines of the two phases are shown in Fig. 3.

The use of reiterative least-square methods to index the powder pattern (*18*, *19*, *20*) of both phases in the cubic, tetragonal, and hexagonal systems was examined with the aid of an IBM-360 computer. However, no unique structural assignments based on small unit cells of one to two formula weights could be made. It is concluded that $(UO_2)Sb_3O_7$ and $Sb_3U_3O_{14}$ possess complex structures which can best be further elucidated by more powerful techniques, such as single-crystal X-ray diffraction and Induced Electron Emission studies.

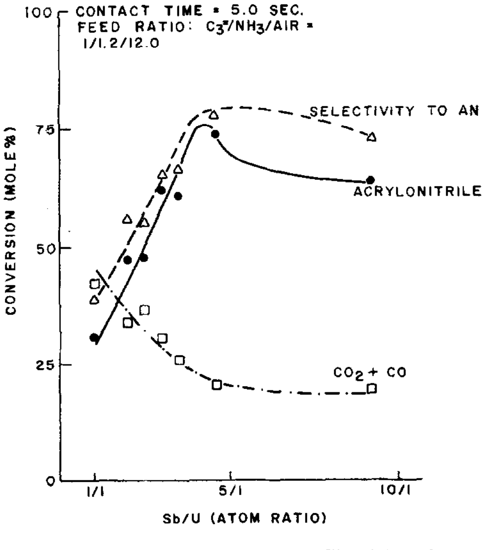

FIG. 2. Activity of unsupported Sb-U-Catalysts at 460°C.

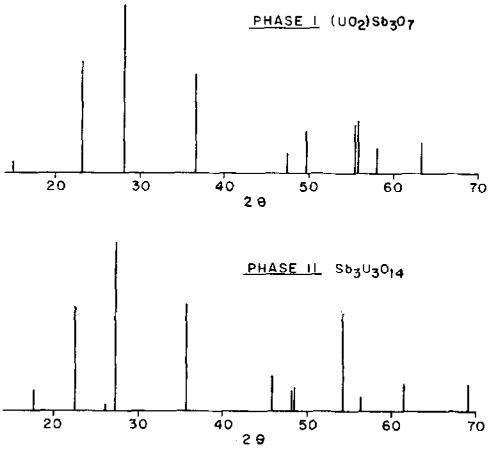

FIG. 3. Major X-Ray diffraction lines of catalyst phases.

In Fig. 4 the relative intensity of the strongest diffraction line of Phase I, Phase II, Sb_2O_4, and U_3O_8 is plotted against Sb/U ratio. A comparison of this figure with Figs. 1 and 2 reveals a significant correlation between the Phase I concentration and the catalytic efficiency for acrylonitrile synthesis.

Low-frequency infrared absorption data for this same series of catalysts identified Phase I as a uranyl antimonate and Phase II as an antimony uranate. The asymmetric $U–O_I$ stretching mode of the linear uranyl structure has been well correlated (*21*, *22*) and occurs near 930 ± 12 cm^{-1} for these catalysts. The intensity of this band increases sharply for Sb/U ratios between 2 and 3 and then levels off (Fig. 5), matching closely the curve obtained from X-ray diffraction data on Phase I concentration (Fig. 4) and the maximum in catalytic activity for acrylonitrile conversion (Figs. 1 and 2). A characteristic band near 740 ± 7 cm^{-1}, assigned to the asymmetric Sb–O stretch (*23*) is also observed over the Sb/U range of 2/1 to 18/1, consistent with the assignment of this phase as a uranyl anti-

TABLE 4

OBSERVED X-RAY POWDER DIFFRACTION LINES OF PHASES I AND II

d(Å)	I/I_1	d(Å)	I/I_1
Phase I $(UO_2)Sb_3O_7$			
5.89	5	2.18	3
4.90	3	1.920	12
3.85	67	1.834	29
3.18	100	1.657	30
2.98[a]	4	1.645	33
2.45	61	1.589	14
2.37	4	1.468	19
2.29	4		
Phase II $Sb_3U_3O_{14}$			
5.04	13	1.703	20
4.72	4	1.691	58
3.95	62	1.630	11
3.41	4	1.627	5
3.26	100	1.622	4
2.98[a]	2	1.617	1
2.93[b]	3	1.576	3
2.79	1	1.564	2
2.59[a]	2	1.550[a]	1
2.51	64	1.536	1
2.44	3	1.529	2
2.35	6	1.524	1
2.33	2	1.518	1
2.16	4	1.507	15
2.14	1	1.500	3
2.06	6	1.458	2
1.975	17	1.416	2
1.936	3	1.360	19
1.886	12	1.341	1
1.875	15	1.325	2
1.819[a]	2	1.317	4
1.799	4	1.296	2
1.767	2	1.274	1
1.735	3	1.271	1

[a] Lines common also to Sb_2O_5 and Sb_6O_{13}.

[b] Lines common also to U_3O_8.

TABLE 5

LOW FREQUENCY INFRARED SPECTRAL ASSIGNMENTS OF U-O$_I$ ASYMMETRIC STRETCH

	Position (cm^{-1})	References
Uranyl Compounds		
$CO_2UO_2(SO_4)_2\cdot 3H_2O$	923	*20*
$KUO_2(NO_3)_3$	943	*20*
$CsUO_2(NO_3)_3$	956	*20*
$CsUO_2Cl_4$	920	*20*
UO_2SO_4	925	*21*
$UO_2(OAc)_2$	940	*21*
$UO_2C_2O_4$	930	*21*
Polyuranates		
$Li_2U_2O_7$	805	*23*
$Na_2U_2O_7$	819	*23*
$K_2U_2O_7$	822	*23*
$Rb_2U_2O_7$	822	*23*
$Cs_2U_2O_7$	825	*23*
Pb_2U_7O	828	[a]
Monouranates		
α-Na_2UO_4	775	*23*
β-Na_2UO_4	745	*23*
K_2UO_4	732	*23*
Rb_2UO_4	726	*23*
Cs_2UO_4	727	*23*
Sb-U Oxides, Sb/U atom ratio		
18.4/1	932	[b]
9.2/1	932	[b]
4.6/1	930	[b]
3.5/1	930	[b]
3.0/1	930	[b]
2.5/1	920	[b]
2.0/1	920	[b]
1.0/1	845	[b]
1.0/1.5	843	[b]
1.0/3	845	[b]
1.0/4.6	845	[b]
1.0/9.2	735	[b]
1.0/18.4	735	[b]
α-U_3O_8	735	*24* [b]

[a] Commercial sample (Alpha Inorganics) run at this laboratory.

[b] This work.

monate. From the X-ray and stoichiometry, the composition is $(UO_2)Sb_3O_7$. Both the 930 cm^{-1} and the 740-cm^{-1} bands disappear at lower Sb/U ratios.

At a catalyst composition of 1 Sb/1 U, a unique band appears in the low-frequency infrared spectrum at 845 cm^{-1}. By analogy to literature references (*24*, *25*) this is assigned to the U–O stretch in a uranate structure. Since the X-ray data established that Phase II is most concentrated at a 1 Sb/1 U ratio (Fig. 4), it is concluded that Phase II is an antimony uranate of composition $Sb_3U_3O_{14}$ (X-ray and stoichiometry).

The low-frequency infrared data are given in Table 5. A plot of the U–O stretching frequency versus the Sb/U ratio is shown in Fig. 6 and illustrates clearly the change in structure (e.g., U–O bond lengths)

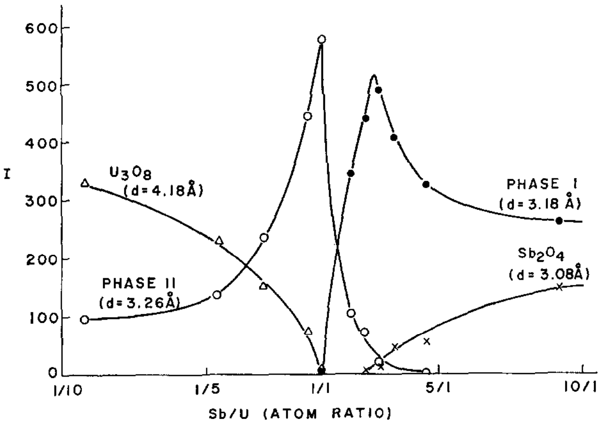

Fig. 4. X-Ray diffraction.

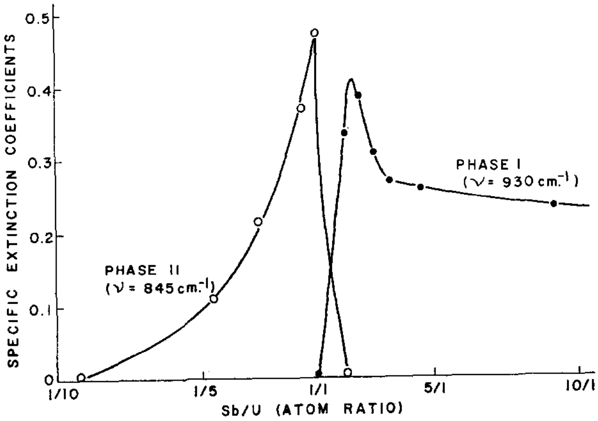

Fig. 5. Low-frequency infrared.

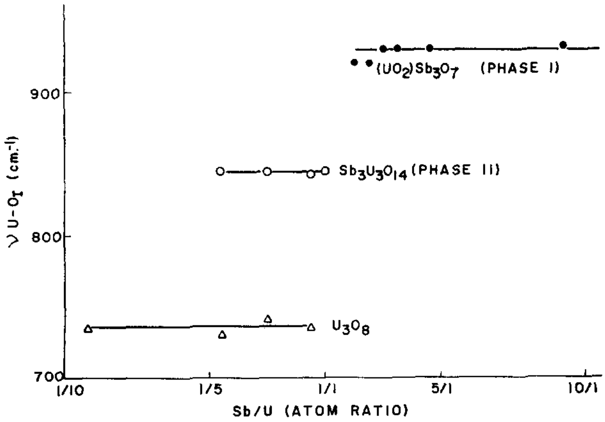

Fig. 6. U-OI stretching frequency as a function of Sb/U ratio.

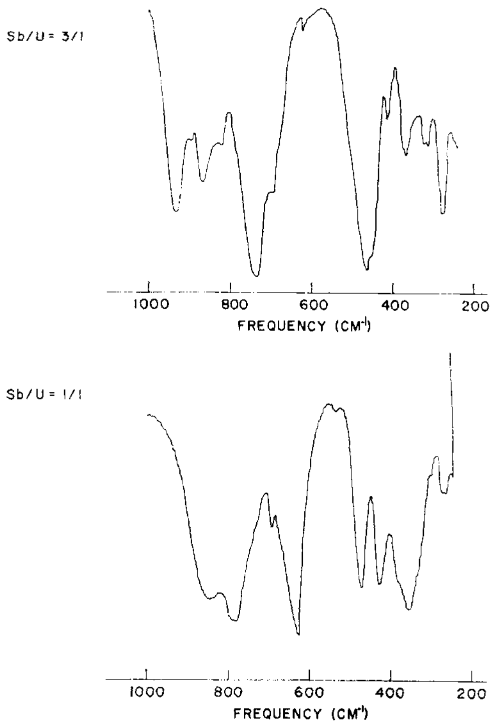

Fig. 7. Low-frequency infrared spectra.

from a uranyl antimonate to an antimony uranate in going from Phase I to Phase II, and finally to U_3O_8 as more uranium is added to the preparations. The distinctive low-frequency spectra for Phase I and Phase II are shown in Fig. 7.

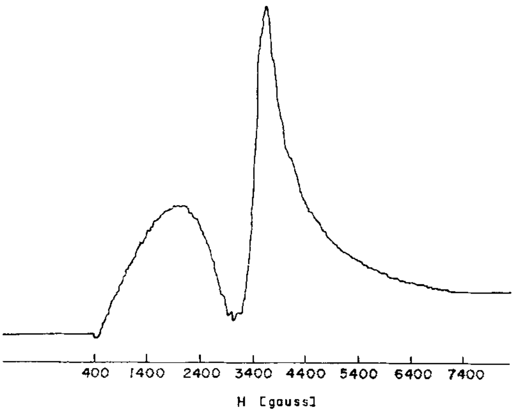

Fig. 8. ESR spectrum of 2 Sb/1 U catalyst composition.

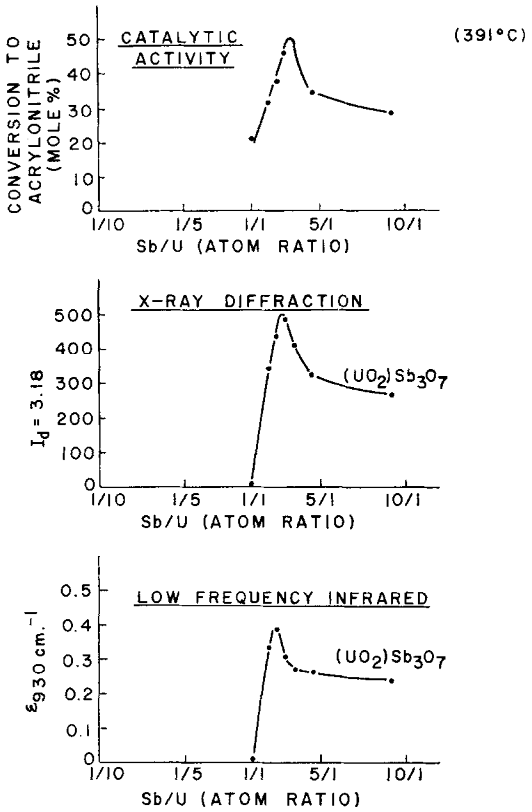

Fig. 9. Correlation between structure and selective catalytic activity.

A preliminary study of the unsupported catalysts with ESR showed unpaired electrons over the entire range of compositions investigated. A broad line at $g = 2.03$ is found when Phase II is present and peaks at 1 Sb/1 U. It is assigned to U^{5+}. A much sharper line at $g = 2.003$ correlates with Phase I concentration. Assignment of this signal is not complete at present. An ESR spectrum of a 2 Sb/1 U composition containing both phases is shown in Fig. 8.

While no firm correlation can be derived at present between ESR and catalytic behavior of the solids investigated, there is an excellent correlation between catalysis and specific bulk crystalline phases (i.e., uranyl antimonate) as determined by X-ray and low-frequency infrared (Fig. 9). The surface of this $(UO_2)Sb_3O_7$ phase is a superior catalyst in terms of activity and selectivity for the ammoxidative synthesis of acrylonitrile. It possesses the appropriate metal–oxygen bond energies and oxygen spatial arrangement for the selective ammoxidation of propylene. The importance of these factors in oxidative catalysis has been recognized by several investigators for some time (*26–31*).

Bench scale fluidized-bed performance of the optimized form of the catalyst was determined using the silica-supported preparation described in the experimental section. The conditions were as follows:

Catalyst wt.	650 g
Particle size range	+88 μ, 15 wt % −44 μ, 30 wt %
Reaction temperature	482°C
Reaction pressure	2 psig
Superficial contact time	8.0 sec
Reactant feed rates (St. cu ft/hr)	Propylene, 0.281 Ammonia, 0.337 Air, 3.09
Prerun	30 min
Recovery run	30 min

Total recovered carbon products accounted for 98.2% of the carbon fed as propylene. The following conversions were found, based on propylene carbon fed:

Acrylonitrile	82.1%
HCN	5.7%
Acetonitrile	Trace
Acrolein	Trace
CO_2	6.7%
CO	3.4%
Unreacted propylene	0.3%
Unreacted ammonia (% of feed)	21.1%

It is clear, therefore, that the effectiveness of this novel uranium–antimony oxide catalyst in the snythesis of acrylonitrile is related to complex and discrete crystalline structures which are not mere mixtures of simple oxides. Commercialization of the catalyst has been realized, resulting in a more efficient, direct oxidative conversion of propylene to acrylonitrile.

ACKNOWLEDGMENTS

The authors gratefully acknowledge the contributions of Dr. D. D. Suresh for catalyst synthesis and discussions of results; R. A. Gerron and Professor C. Knox. (Case-WRU) for assistance with X-ray data; J. A. Rygalski, M. A. Hazle, and J. G. Grasselli for IR results; Dr. E. C. Hughes and The Standard Oil Company (Ohio) for continued interest in this investigation.

REFERENCES

1. IDOL, J. D., JR., U. S. Patent 2,904,580, Sept. 15, 1959 [to The Standard Oil Company (Ohio)].
2. VEATCH, F., CALLAHAN, J. L., IDOL, J. D., JR., AND MILBERGER, E. C., *Chem. Eng. Prog.* **56,** 65 (1960).
3. CALLAHAN, J. L., FOREMAN, R. W., AND VEATCH, F., U. S. Patent 3,044,966, July 17, 1962 [to The Standard Oil Company (Ohio)].
4. VEATCH, F., CALLAHAN, J. L., IDOL, J. D., JR., AND MILBERGER, E. C., *Hydrocarbon Process. Petroleum Refiner* **41,** 187 (1962).
5. ADAMS, C. R., AND JENNINGS, T. J., *J. Catalysis* **2,** 63 (1963).
6. ADAMS, C. R., AND JENNINGS, T. J., *J. Catalysis* **3,** 549 (1964).
7. ADAMS, C. R., *Proc. Intern. Congr. Catalysis, 3rd, Amsterdam, 1964* **1,** 240 (1965).
8. KOLCHIN, I. K., GAL'PERIN, E. L., BOBKOV, S. S., AND MARGOLIS, L. YA., *Kinetika i Kataliz* **6,** 878 (1965).
9. OSTROVSKII, G. M., VOLKOVA, A. N., SADOVSKII, A. S., AND GELBSHTEIN, A. I., *Intern. Chem. Eng.* **5,** 562 (1965).
10. SCHONBECK, R., KONIG, H., KRZEMICKI, K., AND KAHOFER, L., *Angew. Chem., Intern. Ed.* **5,** 642 (1966).
11. VEATCH, F., CALLAHAN, J. L., MILBERGER, E. C., AND FOREMAN, R. W., *Actes Congr. Intern. Catalyse, 2e, Paris, 1960* **2,** 2647 (1961).
12. BLEIJENBERG, A. C. A. M., LIPPENS, B. C., AND SCHUIT, G. C. A., *J. Catalysis* **4,** 581 (1965).
13. BATIST, PH. A., LIPPENS, B. C., AND SCHUIT, G. C. A., *J. Catalysis* **5,** 55 (1966).
14. BATIST, PH. A., KAPTEIJNS, C. J., LIPPENS, B. C., AND SCHUIT, G. C. A., *J. Catalysis* **7,** 33 (1967).
15. CALLAHAN, J. L., AND GERTISSER, B., U. S. Patent 3,198,750, August 3, 1965 [to The Standard Oil Company (Ohio)].
16. CALLAHAN, J. L., AND GERTISSER, B., U. S. Patent 3,308,151, March 7, 1967, [to The Standard Oil Company (Ohio)].
17. CALLAHAN, J. L., AND KNIPPLE, W. R., U. S. Patent 3,341,471, Sept. 12, 1967 [to The Standard Oil Company (Ohio)].
18. HULL, A. W., AND DAVEY, W. P., *Phys. Rev.* **17,** 549 (1921).
19. BELL, J. C., AND AUSTIN, A. E., "Battelle Indexing Charts for Diffraction Patterns of Tetragonal, Hexagonal, and Orthorhombic Crystals." Battelle Memorial Institute, Columbus 1, Ohio, U. S. A.
20. KNOX, C., private communication.

21. McGlynn, S. P., Smith, J. K., and Neely, W. C., *J. Chem. Phys.* **35**, 105 (1961).
22. Hoekstra, H. R., *Inorg. Chem.* **2**, 492 (1963).
23. (a) von Siebert, H., *Z. Anorg. Allgem. Chem.* **301**, 161 (1959). (b) This work.
24. Hoekstra, H. R., *J. Inorg. Nucl. Chem.* **27**, 801 (1965).
25. Carnall, W. T., Walker, A., and Neufeldt, S. J., *Inorg. Chem.* **5**, 2135 (1966).
26. Callahan, J. L., and Grasselli, R. K., *A.I.Ch. E. J.* **9**, 755 (1963).
27. Sachtler, W. H. M., and deBoer, N. H., *Proc. Intern. Congr. Catalysis, 3rd, Amsterdam, 1964* **1**, 252 (1965).
28. Morooka, Y., and Ozaki, A., *J. Catalysis* **5**, 116 (1966).
29. Klier, K., *J. Catalysis* **8**, 14 (1967).
30. Dowden, D. A., *Chem. Eng. Progr. Symp. Series, Kinetics and Catalysis* (No. 73) **63**, 90 (1967).
31. Simons, Th. G. J., Verheijen, E. J. M., Batist, Ph. A., and Schuit, G. C. A., International Oxidation Symposium, San Francisco, 1967, II-29.